iScience, Volume *23*

Supplemental Information

The Symbiotic Relationship between the Neural Retina and Retinal Pigment Epithelium Is Supported by Utilizing Differential Metabolic Pathways

Tirthankar Sinha, Muna I. Naash, and Muayyad R. Al-Ubaidi

Supplemental Information

The symbiotic relationship between the neural retina and retinal pigment epithelium is supported by utilizing differential metabolic pathways

Tirthankar Sinha, Muna I. Naash* and Muayyad R. Al-Ubaidi*

Department of Biomedical Engineering, University of Houston, Houston, TX 77204

Figure S1

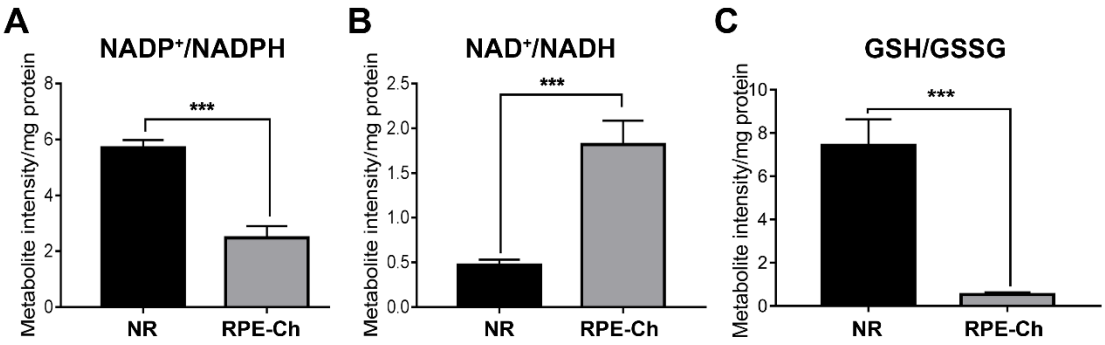

Figure S1. Related to Figure 3. Redox Potential of the RPE and the Retina.

Metabolite ratios exhibiting the redox potential of neural retina and RPE-choroid are shown as scatter plots. Student's two tailed t-test was done for statistical test with *=p<0.05, **=p<0.01, ***=p<0.001, ****=p<0.0001. (NR=Neural retina; RPE-Ch=RPE-choroid).

Figure S2

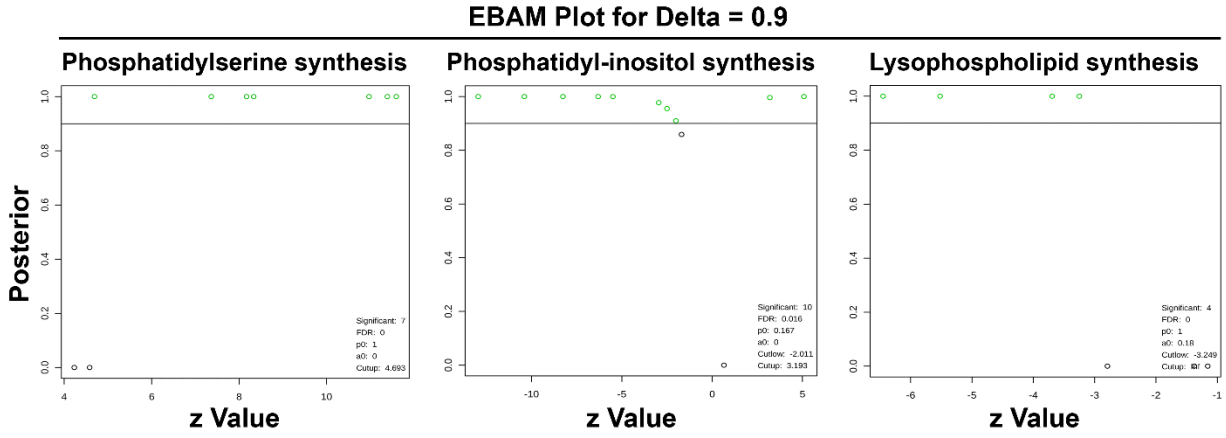

Figure S2. Related to Figure 5. Metabolites of Serine Biosynthetic Pathway are significantly elevated in RPE.

EBAM plot for the metabolites involved in phosphatidylserine biosynthesis, phosphatidylinositol synthesis and lysophospholipid synthesis with a cutoff of 0.9 for delta identifies 7 significant metabolites (features) shown in empty green circles. **(**NR=Neural retina; RPE-Ch=RPE-choroid).

TRANSPARENT METHODS

KEY RESOURCES TABLE

REAGENT or RESOURCE	SOURCE	IDENTIFIER
Antibodies		
Anti-pgd	Proteintech	Cat# 14718-1-AP; RRID:AB_2236801
Anti-pkm2	Cell Signaling Technology	Cat# 4053, RRID:AB_1904096
Anti-phgdh	Proteintech	Cat# 14719-1-AP, RRID:AB_2283938
Anti-psat1	Proteintech	Cat# 10501-1-AP, RRID:AB_2172597
Anti-mdh1	Proteintech	Cat# 15904-1-AP, RRID:AB_2143279
Anti-citrate synthase	Proteintech	Cat# 16131-1-AP, RRID:AB_1640013
Anti-aconitase	Proteintech	Cat# 11134-1-AP, RRID:AB_2289288
Anti-sdh	Abcam	Cat# ab14715, RRID:AB_301433
Anti-mdh2	Proteintech	Cat#15462-1-AP
Anti-sgms1	Proteintech	Cat# 19050-1-AP, RRID:AB_2188417
Anti-beta actin	Abcam	Ab8227;RRID:AB_2305186
Critical Commercial Assays		
NADP/NADPH quantitation assay kit	Sigma-Aldrich	MAK038
Experimental Models: Organisms/Strains		
C57BL/6 mice	(Kelley et al., 2017)	N/A

EXPERIMENTAL MODEL AND SUBJECT DETAILS

Strain/Genetic Makeup of Mice

Animal experiments were approved by the University of Houston Institutional Animal Care and Use Committee (IACUC) and adhered to recommendations in NIH Guide for the Care and Use of Laboratory Animals and the Association for Research in Vision and Ophthalmology. All mice were on C5BL/6J background (C57BL/6- 129S1/SvImJ strain) and were genotyped for and found to be negative for both the *rd8* allele (Chen et al., 2013) and the RPE 65 Leu450Met variant (Danciger et al., 2000; Kim et al., 2004). Animals were reared under cyclic light conditions (12 hours L/D, ~30 lux) and fed with normal chow diet (5053 irradiated Pico Lab Rodent Diet). All animals were between 6-7 weeks of age and the gender distribution was equivalent across all groups.

METHOD DETAILS

Tissue Collection

All mouse protocols adhered to guidelines published by NIH and the Association for Research in Vision and Ophthalmology (ARVO) and were approved by institutional IACUC.

Due to the tight interactions between the neural retina and the retinal pigment epithelium, careful attention was placed on tissue extraction. Following intramuscular injection of 85 mg/kg ketamine and 14 mg/kg xylazine, degree of anesthesia was determined by toe pinching and when mice were fully under, the next steps was undertaken. A disposable surgical knife was used to slit the cornea and lens was extracted. Using curved tweezers, the eye cup was squeezed to obtain the neural retina, which was immediately frozen in liquid nitrogen until use. The remaining eye cup was obtained by cutting with a surgical scissors at the optic nerve and the animal was euthanized. While paying careful attention, the remaining tissue in the back of the eyecup was scraped, with the aid of a dissection microscope, using a curved tweezer, rinsed quickly in phosphate buffer saline (pH=7.4) and immediately frozen in liquid nitrogen. Although careful attention was paid to ensure no scleral tissue was obtained with the scraped tissue, there is the potential of obtaining the choroid

with the retinal pigment epithelium. Therefore, that portion of the eye was termed retinal pigment epithelium-choroid (RPE-choroid) throughout the text.

Tissue was extracted from anesthetized mice rather than euthanized by carbon dioxide to eliminate the potential of effects on tissue metabolic activity resulting from acidification by carbon dioxide. The maintain freshness of tissue, the entire extraction process did not exceed 3 minutes. All samples were thereafter maintained in -80ºC until processed. Six neural retinal samples and subsequent six RPE-choroid samples from six non-littermate animals were pooled and considered as a single 'n' value for neural retina and RPE-choroid. The neural retina groups had a total 'n' value of 8 and the RPE-choroid group had 'n' value of 9. In order to account for minimal effect of outer segment phagocytosis by RPE-choroid, all tissues were collected between 1-3pm, i.e. at the middle of the light cycle. Further, to normalize all animals to steady state metabolite levels and to account for differential feeding, all animals were fasted for 5-6 hours prior to tissue collection.

Metabolomics sample preparation and analysis

Extraction

Several recovery standards were added prior to the first step in the extraction process for quality control purposes. In order to increase maximum yield, methanol extraction was done prior to analysis. To remove protein, dissociate small molecules bound to protein or trapped in the precipitated protein matrix, and to recover chemically diverse metabolites, proteins were precipitated with methanol under vigorous shaking for 2 min followed by centrifugation. The resulting extract was divided into five fractions: two for analysis by two separate reverse phase (RP)/UPLC-MS/MS methods with positive ion mode electrospray ionization (ESI), one for analysis by RP/UPLC-MS/MS with negative ion mode ESI, one for analysis by HILIC/UPLC-MS/MS with negative ion mode ESI, and one sample was reserved for backup. Post removal of the organic solvent, the sample extracts were stored overnight under nitrogen before preparation for analysis.

Measurements

All methods utilized a Waters ACQUITY ultra-performance liquid chromatography (UPLC) and a Thermo Scientific Q-Exactive high resolution/accurate mass spectrometer interfaced with a heated electrospray ionization (HESI-II) source and Orbitrap mass analyzer operated at 35,000

mass resolution. The sample extract was dried then reconstituted in solvents compatible to each of the four methods. Each reconstitution solvent contained a series of standards at fixed concentrations to ensure injection and chromatographic consistency. One aliquot was analyzed using acidic positive ion conditions, chromatographically optimized for more hydrophilic compounds. In this method, the extract was gradient eluted from C18 column (Waters UPLC BEH C18-2.1 x 100 mm, 1.7 µm) using water and methanol, containing 0.05% perfluoropentanoic acid (PFPA) and 0.1% formic acid (FA). Another aliquot was also analyzed using acidic positive ion conditions; however it was chromatographically optimized for more hydrophobic compounds. In this method, the extract was gradient eluted from the same afore mentioned C18 column using methanol, acetonitrile, water, 0.05% PFPA and 0.01% FA and was operated at an overall higher organic content. Another aliquot was analyzed using basic negative ion optimized conditions using a separate dedicated C18 column. The basic extracts were gradient eluted from the column using methanol and water, however with 6.5mM Ammonium Bicarbonate at pH 8. The fourth aliquot was analyzed via negative ionization following elution from a HILIC column (Waters UPLC BEH Amide 2.1x150 mm, 1.7 µm) using a gradient consisting of water and acetonitrile with 10mM Ammonium Formate, pH 10.8. The MS analysis alternated between MS and data-dependent MS^n scans using dynamic exclusion. The scan range varied slighted between methods but covered 70-1000 m/z.

Compounds were identified by comparison to library entries of purified standards or recurrent unknown entities. Peaks were quantified using area-under-the-curve. For studies spanning multiple days, a data normalization step was performed to correct variation resulting from instrument inter-day tuning differences. Biochemical data for each metabolite was further normalized to protein concentration measured by Bradford assay to account for differences in metabolite levels due to differences in the amount of material present in each sample.

Quality control

Several types of controls were analyzed in concert with the experimental samples: a pooled matrix sample generated by taking a small volume of each experimental sample (or alternatively, use of a pool of well-characterized plasma) served as a technical replicate throughout the data set; extracted water samples served as process blanks; and a cocktail of quality control standards that were carefully chosen not to interfere with the measurement of endogenous compounds were spiked into every analyzed sample, allowed instrument performance monitoring and aided

chromatographic alignment. Instrument variability was determined by calculating the median relative standard deviation (RSD) for the internal standards that were added to each sample prior to injection into the mass spectrometers. Overall, process variability was determined by calculating the median RSD for all endogenous metabolites (i.e., non-instrument standards) present in 100% of the technical replicates of pooled samples. Internal standards reflected instrument variability of only 6% median RSD, while endogenous metabolites reflected a total process variability of only 2% median RSD. Experimental samples were randomized across the platform run with QC samples spaced evenly among the injections.

Microarray Data Analysis

The NCBI GEO (GNF Mouse GeneAtlas V3) was used to access the *Mus musculus* GSE10246 microarray gene expression dataset as well as the probe IDs for all the genes used in the dataset. The strain (C57BL6/J) and age of the animals (6-9 weeks) were similar to our rest of the study. The data was filtered by specifically selecting for retina and RPE-choroid tissue expression and the heat map was generated from the resulting values of the selected genes via heat map 2.0 package in R-studio with 2 replicates for each sample.

NADP/NADPH measurements

Measurements were done using the Sigma Aldrich NADP/NADPH quantitation kit, as per manufacturer's instructions on freshly collected neural retina and RPE-choroid.

Immunoblotting

Mouse neural retinas and RPE-choroid were collected as explained earlier under "Tissue Collection" in methods and homogenized using a handheld motor and pestle tip in RIPA lysis buffer containing 0.1% Triton X-100 and a complete protease inhibitor cocktail. Following 1 hour incubation at 4°C, the insoluble material was separated via centrifugation at 14,000xg for 15minutes. The supernatant was transferred to new tube and protein concentration were determined via Bio-Rad Bradford Assay. Cell lysates (20µg protein) were incubated for 30minutes at room temperature in Laemmli buffer containing beta-mercaptoethanol and then size fractionated via 10% SDS-PAGE. Images were captured using a Bio-Rad ChemiDoc MP Imaging System equipped with Image Lab 5.0 software. Gels were then transferred to PVDF membranes and

immunoblotting was carried out as previously described (Kelley et al., 2017). After imaging the blot for the desired proteins, the blot was dried and reimaged to ensure there was no residual signal left. The same blot was blocked again with 5% milk and re-probed with the primary antibody against the desired protein. This was repeated for all the proteins. Using the same immunoblot repeatedly allowed us to quantify the different proteins with less variability.

QUANTIFICATION AND STATISTICAL ANALYSES

Data Transformation

After log transformation and imputation of missing values, if any, with the minimum observed value for each compound, ANOVA contrasts were used to identify metabolites that differed significantly ($p \leq 0.05$), between experimental groups. An estimate of the false discovery rate (q-value) was also calculated to take into account the multiple comparisons that normally occur in metabolomic-based studies.

Data Visualization

Feature scaling was done for each metabolite across all groups to set the median equal to 1. For data visualization, scatter plot was used so that the individual measurements can be seen. All data were normalized to protein levels as described in methods section.

SUPPLEMENTAL REFERENCES

Chen, X., Kezic, J., Bernard, C., and McMenamin, P.G. (2013). Rd8 mutation in the Crb1 gene of CD11c-eYFP transgenic reporter mice results in abnormal numbers of CD11c-positive cells in the retina. J Neuropathol Exp Neurol *72*, 782-790.

Danciger, M., Matthes, M.T., Yasamura, D., Akhmedov, N.B., Rickabaugh, T., Gentleman, S., Redmond, T.M., La Vail, M.M., and Farber, D.B. (2000). A QTL on distal chromosome 3 that influences the severity of light-induced damage to mouse photoreceptors. Mamm Genome *11*, 422-427.

Kelley, R.A., Al-Ubaidi, M.R., Sinha, T., Genc, A.M., Makia, M.S., Ikelle, L., and Naash, M.I. (2017). Ablation of the riboflavin-binding protein retbindin reduces flavin levels and leads to progressive and dose-dependent degeneration of rods and cones. J Biol Chem *292*, 21023-21034.

Kim, S.R., Fishkin, N., Kong, J., Nakanishi, K., Allikmets, R., and Sparrow, J.R. (2004). Rpe65 Leu450Met variant is associated with reduced levels of the retinal pigment epithelium lipofuscin fluorophores A2E and iso-A2E. Proc Natl Acad Sci U S A *101*, 11668-11672.